

RSC Advances



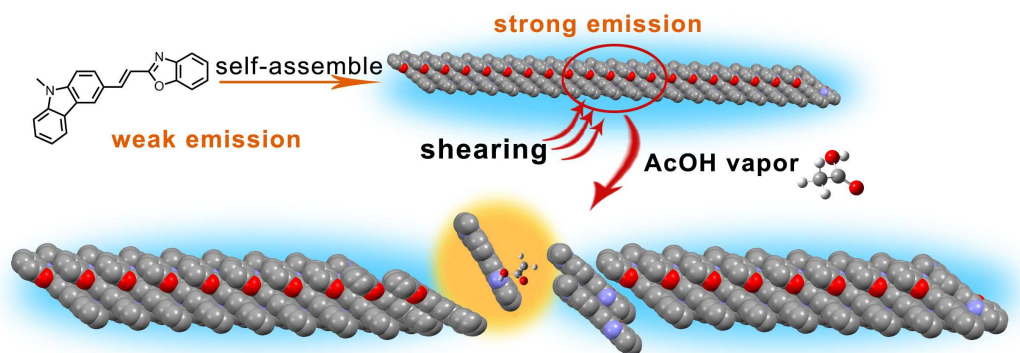
This is an *Accepted Manuscript*, which has been through the Royal Society of Chemistry peer review process and has been accepted for publication.

Accepted Manuscripts are published online shortly after acceptance, before technical editing, formatting and proof reading. Using this free service, authors can make their results available to the community, in citable form, before we publish the edited article. This *Accepted Manuscript* will be replaced by the edited, formatted and paginated article as soon as this is available.

You can find more information about *Accepted Manuscripts* in the [Information for Authors](#).

Please note that technical editing may introduce minor changes to the text and/or graphics, which may alter content. The journal's standard [Terms & Conditions](#) and the [Ethical guidelines](#) still apply. In no event shall the Royal Society of Chemistry be held responsible for any errors or omissions in this *Accepted Manuscript* or any consequences arising from the use of any information it contains.

Graphic abstract



The nanofibers of carbazole-based benzoxazole derivative have enhanced emission and exhibited an isothermal reversible mechanochromism. Moreover acetic acid vapor may selectively act as stabilizer and developer to retain the information given by mechanical force.

Cite this: DOI: 10.1039/c0xx00000x

www.rsc.org/xxxxxx

ARTICLE TYPE

Response of Strong Fluorescence Carbazole-based Benzoxazole Derivative to External Force and Acid Vapor

Pengchong Xue,* Boqi Yao, Panpan Wang, Jiabao Sun, Zhenqi Zhang, Ran Lu*

Received (in XXX, XXX) Xth XXXXXXXXX 20XX, Accepted Xth XXXXXXXXX 20XX

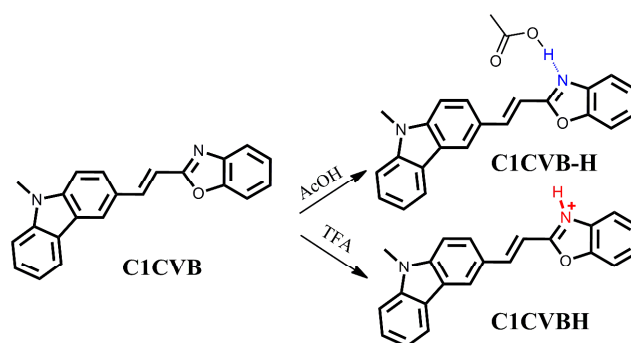
DOI: 10.1039/b000000x

A carbazole-based D- π -A benzoxazole derivative was found to self-assemble into long fibers and possessed enhanced emission because of the presence of J-aggregate. These fibers exhibited distinct responses to volatile acid vapors. Strong acid, such as HCl and TFA vapors would destroy the molecular packing in fiber and induced the color change in fluorescence. On the other hand, fibers had no response to HOAc vapor as weak acid. Moreover, the fibrous film exhibited an isothermally reversible piezofluorochromism. Its blue fluorescence converted to blue-green one upon mechanical force stimulus and then was restored spontaneously at room temperature. More importantly, the response of fibrous film to HOAc vapor was controlled by mechanical stimulus. The colorless ground film could easily absorb HOAc vapor and emitted orange fluorescence. Moreover, such colored film could not self-heal, but get back to colorless and blue emission upon heating. Thus, acetic acid vapor may selectively act as stabilizer and developer to retain the information given by mechanical force. These results show that stimuli response of organic nanofibers could be adjusted and controlled by mechanical stimulus, and vice versa.

Introduction

Stimulus-active organic functional materials have gained considerable attention from scientists.¹ These materials can change their physical or chemical characteristics upon exposure to particular external stimuli (e.g., heat, electricity, light, force, magnets and other chemical stimuli). Among these materials, attention is given to organic molecules with strong emissions in solid state as new functional materials in electronics, photo devices, and solid lasers.² These strong emissive fluorophores are also used as smart materials to selectively detect chemical reagents such as explosives,³ organic amines,⁴ acidic gases,⁵ metal ions,⁶ and oxygen.⁷ The responsive characteristics of the fluorophores to these chemical reagents are strongly affected by fluorophore morphologies. For example, self-assembled fluorescent fibers used as sensing materials to detect explosives and organic amine require small diameter to obtain large surface area. Only ultrathin polymer films have rapid responses and low detection limits to explosive vapor because vapor molecules are easy to absorb and diffuse in thin films.⁸

Solid state emission reflects the molecular structure and arrangement in the solid state.⁹ Molecular orientation and intermolecular interaction are perturbed by mechanical forces such as shearing, grinding, tension, or hydrostatic pressure.¹⁰ Thereafter, a drastic emission color change presents piezofluorochromism (PFC). Several types of organic molecules that exhibit PFC behavior have been designed and synthesized. Numerous studies have suggested that tetraphenylethene, triphenylethene, and 9,10-bis-vinyl anthracene derivatives or D-



Scheme 1. the molecular structures of C1CVB, C1CVB-H and C1CVBH.

π -A emissive molecules contribute to fluorescence changes under pressure.¹¹ Because external force stimuli can change the morphologies and stacking model of organic molecules, we attempt to determine whether PFC materials exhibit different responses to another stimuli before and after force stimuli, or whether extra stimulus regulates the PFC behavior of materials.

Herein, we used a D- π -A benzoxazole derivative, namely, C1CVB,¹² which exhibited an isothermally reversible piezofluorochromism, to study how extra stimuli affect its PFC. It was found that molecules can self-assemble into long fibrous aggregates in solvents and exhibit aggregation-induced emission. The nanofibers may selectively respond to volatile acid vapors according to their acidities. HCl and TFA vapors as strong acid induced color change in fluorescence, but the fibers did not respond to HOAc vapor. More importantly, the ground film changed the emission color from blue-green to orange when exposed to HOAc vapor. Moreover, HOAc-dyed ground film

hold dyed state. This difference in sensing behavior is explored, and the result suggests that the sensing properties of functional materials to external stimuli are significantly adjusted by another stimulus, and vice versa.

5 Results and discussion

C1CVB as colorless needle-like crystal was synthesized by a one-step Knoevenagel reaction (Scheme S1)¹³ and is characterized by elemental analysis, NMR, FT-IR, and MS. The peaks at 8.08 and 7.15 ppm in the ¹H NMR spectra ascribed to the vinyl group protons have a large coupling constant of 16.2 Hz, thus indicating that the vinyl group exhibits a transformation. This finding may be confirmed by a single-crystal structure (vide infra). **C1CVB** easily dissolves in CH₂Cl₂, benzene, toluene, THF and DMF, but has low solubility in cyclohexane, hexane, and polar alcohols at room temperature.

The solutions are weak emissive under excitation. The fluorescence quantum yield (Φ_F) in toluene is 0.01. The Φ_F s in other solvents are also low (Table S1). The average lifetime is 0.95 ns (Fig. S1) in toluene, and the radiative (K_r) and nonradiative (K_{nr}) rates are 0.012 and 1.4 ns⁻¹, respectively. Small K_r and large K_{nr} indicate that the excited molecules are mainly deactivated through the nonradiative process. The intramolecular rotation of single bonds and cis-trans isomerisation of double bond should be responsible to low Φ_F .¹⁴

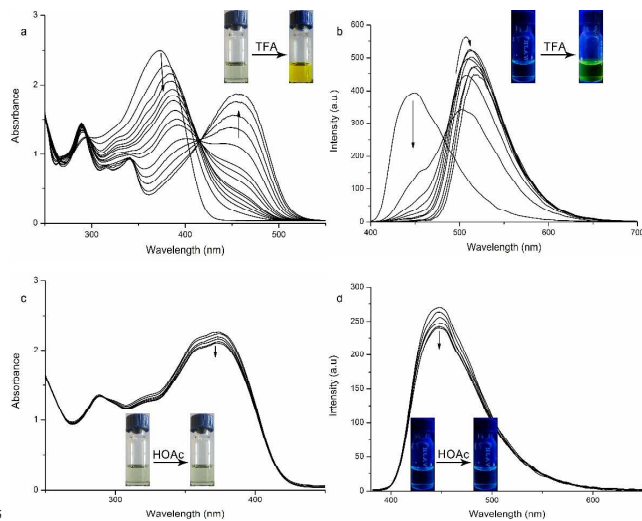


Fig. 1 Absorption and emission spectra of **C1CVB** in CHCl₃ (2×10^{-4} M) upon additional TFA (a and b) and acetic acid (c and d); $\lambda_{em} = 370$ nm.

C1CVB is used as a sensor to detect H⁺ because the benzoxazole moiety can bind a proton to form a cation.¹⁵ Fig. 1a shows that the absorption band of **C1CVB** in CHCl₃ exhibits a continuous bathochromic shift when TFA is added, and a new peak appears at 445 nm. This peak results in a solution color change from yellowish to yellow. The isobestic point is observed at 415 nm, thus implying a reactive equilibrium of two components. The blue emission band at 447 nm upon excitation at 370 nm gradually decreases when TFA is added and an enhanced green emission band emerges at 511 nm (Fig. 1b). Furthermore, the fluorescence spectra of **C1CVB** are more sensitive than the absorption spectra. For example, the fluorescence of the CHCl₃ solution is reduced by almost 70% in the presence of a 2-fold

TFA. A 10-fold TFA almost quenches the emissive peak at 447 nm, but the original absorption ascribed to free **C1CVB** is still obvious at the same TFA concentration (Fig. S2). The increase in solvent polarity induced by TFA addition is responsible for high sensitivity of fluorescence spectrum to TFA because polarity solvent can quench the emission of ICT molecule. Considering the new absorption at 445 nm and the existence of one isobestic point, TFA protonated **C1CVB** in CHCl₃ to form a cation (**C1CVBH**) (Fig. S3). ¹H NMR spectra before and after adding TFA were measured and compared to further understand the interaction between **C1CVB** and TFA. Evident downfield shifts were observed for all protons, particularly the benzoxazole ring and vinyl group when TFA was added. For example, the resonance peaks for H1 and H2 at 8.01 and 7.11 ppm shifts to 8.38 and 7.22 ppm, respectively (i.e., shifts of 0.11 and 0.37 ppm). This result suggests that the proton binding of **C1CVB** ascribes to the protonation of the nitrogen atom in the benzoxazole unit, thus reducing the electron density around all protons and causing downfield shifts in the NMR spectra.^{13,16} The protonation truth also reveals strong acidity of TFA.

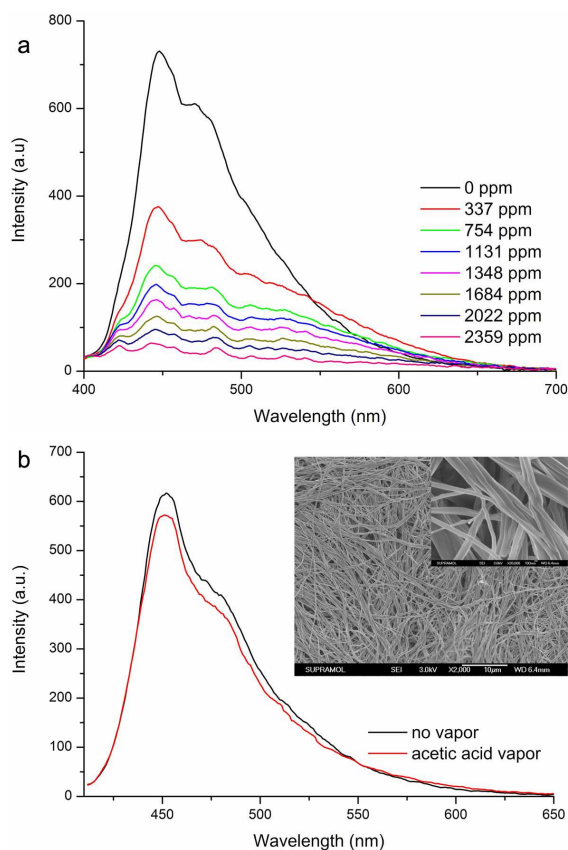


Fig. 2 Fluorescence spectra of **C1CVB** film upon exposure to (a) TFA and (b) acetic acid (saturated) vapors. Inset is SEM image of film.

What will happens if a weak acid such as acetic acid (HOAc) is added? The color of the **C1CVB** CHCl₃ solution was still yellowish even after addition of 50 equiv. HOAc. Only a slight decrease in absorbance is observed when HOAc was added (Fig. 1c), and no shift was observed for the absorption band. The addition of HOAc did not change the fluorescent color either. Fig. 1d shows that the emissive intensity only continues to decrease

when HOAc is added gradually. This spectral change illustrates that HOAc cannot protonate the nitrogen atom of **C1CVB** to form a cation. Moreover, adding 5 equiv. HOAc into the **C1CVB** CDCl₃ solution induces a downshift of all protons, but the shifts are smaller than those when TFA is present (Fig. S3). For instance, the signals for H1 and H2 shift to 8.04 and 7.14 ppm, respectively, meaning a down-field shift of 0.03 ppm for the two protons. These spectral changes suggest a hydrogen bond complex (**C1CVB-H**) of **C1CVB** and HOAc because HOAc has weak acidity. These results clearly illustrate that **C1CVB** in the solution state has different responses to TFA and HOAc because of distinct protonated abilities to **C1CVB**. Therefore, **C1CVB** in solid state is expected to hold distinct responsive behaviors to TFA and HOAc vapors.

As we know, fluorescent nanofibers have been used as sensing materials to detect explosives and organic amines. The thin fibers of **C1CVB** are easily prepared by ultrasound treatment and aging in cyclohexane. The fibrous film is selected to study the response of **C1CVB** to volatile acid vapors. Nanofiber film is prepared as follows. The clear hot cyclohexane solution of **C1CVB** (3.1 mM) was initially treated in an ultrasonic bath until an ivory suspension was observed. A 50 μ l suspension was then dropped on the silica plate surface. A watch glass was used to delay the evaporation of the solvent. After completely removing the solvent, the film sample was obtained. An SEM image of the film shows that **C1CVB** self-assembles into long fibers with diameters of 50 nm to 500 nm (Fig. 2, inset). The fibrous film emits strong fluorescence with an absolute fluorescence quantum yield of 0.71, which is 26 times more than the solution. The time-resolved fluorescence spectrum shows that the fiber has a long fluorescent lifetime (2.3 ns), large K_f (0.32 s⁻¹), and small K_{nr} (0.13 s⁻¹). The obvious red shift in the absorption spectrum of the fibrous film relative to that in the cyclohexane solution suggests the formation of J-aggregation in nanofiber (Fig. S4).¹⁷ Therefore, the enhanced emission is ascribed to the J-aggregation formation and restriction of intramolecular rotation.¹⁸

The solution has a favorable response to proton. The behavior of fibrous film in response to volatile acid is then studied. The colorless film rapidly converted to red when exposed to saturated TFA vapor, the fluorescence color changed from bright blue to red, and emissive intensity decreased. As shown in Fig. 2a, the fibrous film has a maximum emission in 452 nm with some shoulder peaks, ascribing to vibrational bands. The fluorescence is quenched by 48% under TFA vapor of 337 ppm. At this time, the film still emits blue fluorescence. Increasing the TFA concentration will further quench the film emission. The film fluorescence is reduced by almost 92% when exposed to TFA vapor (2359 ppm), and the film emits a weak red fluorescence. A weak new peak at ca. 470 nm in the absorption spectrum is observed (Fig. S5a) and the original absorption band is still present and enough strong. This spectral change indicates that **C1CVB** could bind TFA even in a solid state although all molecules didn't form **C1CVBH** at this concentration of TFA. However, the colorless film maintains its color and blue fluorescence when exposed to saturated acetic acid vapor. Fig. 4 shows that HOAc vapor leads to slight decrease in emissive intensity. No obvious change in the absorption spectra of film is observed after exposure to HOAc vapor (Fig. S5b). Moreover, we observed that HCl vapors with strong acidity had the same response behavior as that of TFA (Fig. S6a). Therefore, the different responses of **C1CVB** fibrous film to TFA and HOAc

should be attributed to the distinct acidities of TFA and HOAc; this result is similar to the phenomenon observed in the solution.

Molecular arrangements in **C1CVB** crystal are investigated by using single-crystal X-ray analysis to obtain insight into the different responses of fibrous film to TFA and HOAc. Crystals and fibers have the same XRD patterns, indicating their same packing model.¹² In the rod-like crystal, 1D π - π molecular packing occurs wherein the distance between two adjacent **C1CVB** molecules is 3.56 Å and the sliding angle is 34.4° (Fig. S7a). This result clearly indicates the formation of J-aggregation in the crystals, verifying the result from UV-vis spectra.¹⁹ Many 1D J-aggregates are stacked together by intermolecular weak interactions (Fig. S7b). This close intermolecular stacking does not hold a large space in crystal cell enough to allow HOAc molecules to diffuse into the fiber interior and form a hydrogen complex. Moreover, a few polar benzoxazole groups are exposed on the fiber surface because cyclohexane is a nonpolar solvent and N atom of benzoxazole moiety locates at the center of whole molecule. Thus, only a small amount of HOAc molecules can absorb on some sites, wherein the nitrogen atoms of benzoxazole units are located at the fiber's surface, to form hydrogen bond complexes (**C1CVB-H**). Consequently, the fluorescence of fibrous film is slightly quenched by the HOAc vapor even at a high concentration. When TFA and HCl meet with N atoms of benzoxazole moieties the strong acidity of TFA and HCl causes the nitrogen atom to be protonated and transferred into a cation, which then destroys the close packing in nanofibers. As a result, other TFA or HCl molecules can diffuse into the fiber interior to form **C1CVBH**, which is why a new absorption peak at 470 nm appeared when the film was exposed to TFA vapor. Such hypothesis can be also confirmed by the observation of XRD spectra. HOAc vapor did not induce any change in XRD spectrum of fibrous film (Fig. S8), but relative weak diffraction peaks in XRD pattern were found when fibrous film was exposed to TFA because **C1CVBH** weakened the order stacking of molecule in nanofibers. Therefore, the fibrous film of **C1CVB** selectively responds to volatile acids according to their acidities.

HOAc vapor is an awkward stimulus to the fibrous film of **C1CVB** because HOAc cannot diffuse freely into fibers. What happens if the intermolecular space is large enough or has a large amount binding sites (N atoms of benzoxazole moieties)? Mechanical stimuli, such as shearing, grinding, rubbing, and static pressure, can convert the crystal phase to amorphous solid or other crystal phases, which is accompanied by color or/and fluorescent color changes and loose or close stacking between molecules. Thereafter, we examined the influence of mechanical stimuli on the responsive behavior of **C1CVB** to volatile acids.²⁰

The ground film is used as a sensor material and is prepared as follows. First, the fibrous thin film is prepared as shown above, and then a shear stress is applied using a spatula to form a thin film. The colorless fibrous film changes to yellowish even though the absorption spectrum of the ground film is similar to the fibrous one (Fig. S9a). Moreover, applying mechanical shearing to the fibrous film causes a fluorescence color change from blue to blue-green. Fig. S9b shows that the ground film possesses a red-shifted and wide emission band with a maximum at 484 nm. Moreover, shearing also induces a decrease in fluorescence intensity. The spectral change implies that **C1CVB** is a piezofluorochromic organic molecule.²¹ The XRD patterns of the fibrous film show many sharp peaks, thus indicating that the fiber is crystalline. By contrast, the ground film becomes amorphous

because of the lack of XRD peaks (Fig. S10).²² No obvious shift in the absorption spectra is observed when shearing is applied, thus suggesting that π - π interactions still exist in the ground sample and that mechanical shearing only promotes disordered small pieces wherein π - π interaction is maintained and a large amount of naked N atoms of benzoxazole units appear. When the ground powder was exposed to CH_2Cl_2 vapor for several seconds, the weak blue-green emission rapidly changed to strong blue one. This process of fluorescence color change can be repeated many times. Moreover, the absorption spectrum and XRD of ground film restored to original one upon fuming, suggesting that the fluorescence change is ascribed to the recovery of crystal state. These spectral changes indicate an obviously reversible MFC behavior. More importantly, we found that the emission of the ground samples recovers spontaneously at room temperature within 20 min (Fig. S11), meaning a self-healing material.²³ This charming self-healing property can be explained by differential scanning calorimetry (DSC) measurements (Fig. S12). Fibrous sample has an endothermic peak at 211 °C, corresponding to melting point, and the DSC curve of ground powder displays two transition peaks. One is melting peak. Another weak and wide exothermic peak at 64 °C should be re-crystallization of ground powders, indicating that the ground powder existed as metastable amorphous phase.²⁴ Low transition temperature is a premise for ground film to recover the fluorescence spontaneously.

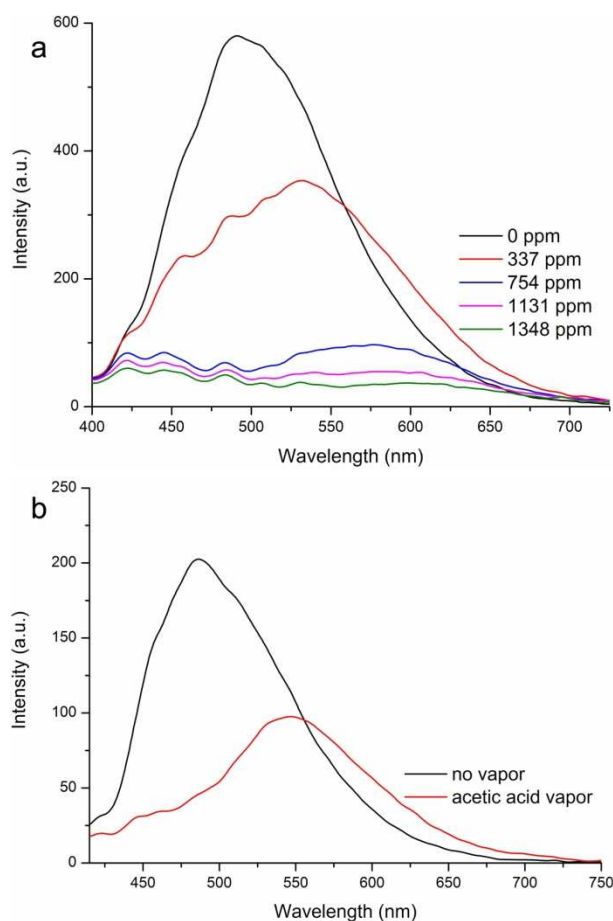


Fig. 3 Fluorescence spectra of ground **C1CVB** films before and after exposure to (a) TFA and (b) HOAc (saturated) vapors.

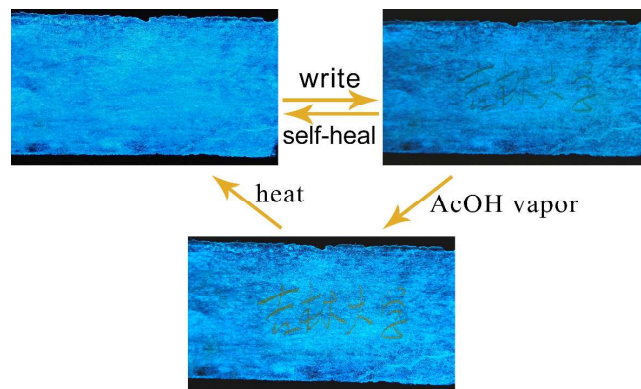


Fig. 4 Photographic images of fibrous film on a piece of weighing paper in response to shearing, HOAc vapor, and heating under UV light (365 nm).

More interestingly, when the ground film was exposed to TFA and HCl vapor, the film color rapidly converted from colorless to orange, and a fluorescence color change from strong blue to weak red was observed. Furthermore, TFA or HCl vapor at low concentrations induce an obvious transformation in fluorescence color (Fig. 3a and S6b). When the TFA concentration is 337 ppm, the ground film converts the fluorescence color from blue-green to green. The maximum emissive peak shifts to 532 nm. It should be noted that several shoulder peaks below 525 nm may be from the molecular emission in crystal state. The increased TFA concentration further quenches film fluorescence, and the emissive peak gradually red shifts. A red emissive band with a maximum of 603 nm is observed as the concentration becomes as high as 1348 ppm. When the HCl vapor was used as a stimulus, the fluorescence color changed from green to orange at a low concentration of 228 ppm, and a red emission ($\lambda_{\text{em}} = 606$ nm) was observed at a high concentration of HCl vapor (Fig. S6b). Furthermore, an obvious color change was observed for the ground film when exposed to TFA or HCl vapor. A new absorption band with a maximum of 427 nm appeared and the original absorption band disappeared (Fig. S13a), thus indicating that **C1CVB** transforms into **C1CVBH**. These spectral changes in the ground film when exposed to TFA and HCl clearly illustrates that **C1CVB** molecules can easily bind protons relative to the fibrous film because many naked binding sites exist in ground film.

When a ground film was selected as the sensing film to evaluate its response to acetic acid, a rapid and obvious color change from blue-green to yellow in fluorescence was found. The maximum emissive peak is at 547 nm (Fig. 3b). The yellowish ground darkens in color when exposed to saturated HOAc vapor. The absorption spectrum of ground film after exposure to HOAc vapor is similar to fibrous film (Fig. S13b). Moreover, some diffraction peaks appeared after fuming by HOAc vapour (Fig. S10), suggesting that HOAc does not promote **C1CVBH** formation and the fuming of HOAc vapor induced many molecules in ground film to recrystallize and form order aggregates.²⁵ At the same time, there exist a significant number of **C1CVB-H** because of the existence of a large amount of naked binding sites in ground film. Thus, the distinct responsive behavior of **C1CVB** films to HOAc vapor is caused by different stacking manners between sensing molecules. This result also reveals that the response of a sensing material to external stimulus can be controlled by other stimuli.

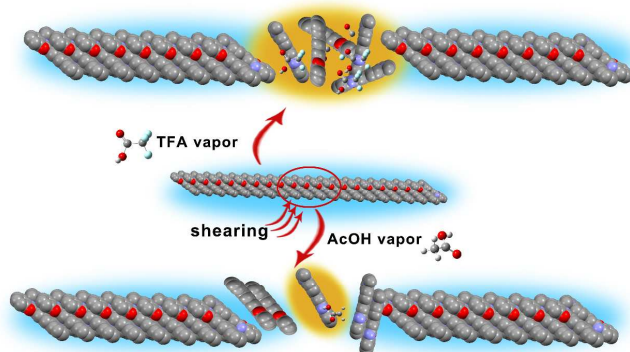


Fig. 5 Schematic of patterned films in response to TFA vapor at a low concentration and HOAc.

The fibrous film exhibits different features in response to volatile acid vapor under external mechanical force stimulus. Thus, volatile acid vapor can adjust the piezochromism of these fibrous films. Fig. 4 shows that a blue-green fluorescent pattern is easily obtained by writing with a stainless steel bar. The pattern exhibits a poor contrast to blue fluorescent background because of the small spectral shift after grinding. An orange fluorescent pattern is observed when the patterned film is exposed to saturated HOAc vapor. The fluorescent background remains blue because HOAc as a weak acid is absorbed preferentially on the **C1CVB** molecules in the patterned region (Fig. 5). Thus, HOAc vapor can be an alternative approach to realize a high contrast piezofluorochromism in fluorescent color. Additional, it was found that HOAc-dyed pattern did not disappeared spontaneously at room temperature even after several days or upon fuming by organic solvents. So, HOAc vapor may be regarded as stabilizer and developer to retain the information of pattern. It is notable that HOAc-dyed pattern may be erased through heating for 30 min at 100 °C, and recovered film can be used repeatedly (Fig. 4). When saturated TFA vapor acted as an assistant stimulus, the whole fibrous film became red (Fig. S14) because a large amount of **C1CVBH** formed. However, exposing the patterned film to TFA vapor with a low concentration (i.e., 1000 ppm for 2 s) caused a yellow pattern, emitting orange fluorescence, and an unpatterned background is still colorless and has a blue emission. This phenomenon is because the naked **C1CVB** molecules quickly bind TFA molecules relative to those in the fibers (Fig. 5).

Conclusions

A carbazole-based benzoxazole derivative may self-assemble into long fibers and has enhanced emission. The fibrous film exhibited piezofluorochromism and changed its fluorescence from blue to blue-green by grinding. Moreover, ground film could self-heal and restored blue fluorescence spontaneously at room temperature because of low recrystallization temperature. The nanofibers did not respond to HOAc vapor. However, the ground film changed the emission color from blue-green to orange when exposed to HOAc vapor because a large amount of naked binding sites existed after grinding. HOAc-dyed ground film held dyed state until heating at a high temperature was applied. The results show that the material response to stimuli can be adjusted by other stimuli, and one may regulate material features by applying multiple stimuli.

Acknowledgements

This work was financially supported by the National Natural Science Foundation of China (21103067, and 21374041), the Youth Science Foundation of Jilin Province (20130522134JH), the Open Project of the State Key Laboratory of Supramolecular Structure and Materials (SKLSSM201407), the Open Project of State Laboratory of Theoretical and Computational Chemistry (K2013-02).

Notes and references

- ⁵⁵ ^a State Key Laboratory of Supramolecular Structure and Materials, College of Chemistry, Jilin University, Changchun, P. R. China, E-mail: xuepengchong@jlu.edu.cn; luran@mail.jlu.edu.cn
- [†] Electronic Supplementary Information (ESI) available: [experimental section, Time-resolved fluorescence, NMR, UV-vis absorption and fluorescence spectra of solutions or films spectra, molecular packing in crystal, XRD patterns and DSC curves]. See DOI: 10.1039/b000000x/
- [‡] Footnotes should appear here. These might include comments relevant to but not central to the matter under discussion, limited experimental and spectral data, and crystallographic data.
- (a) M. K. Beyer, H. Clausen-Schaumann, *Chem. Rev.* 2005, **105**, 2921–2948; (b) L. R. Xia, X. Xie, W. Ju, Q. Wang, L. Chen, *Chem. Nat. Commun.* 2013, **4**, 2226–2237; (c) H. Li, D. X. Chen, Y. L. Sun, Y. B. Zheng, L. L. Tan, P. S. Weiss, Y. W. Yang, *J. Am. Chem. Soc.* 2013, **135**, 1570–1576; (d) Q. Benito, X. F. Le Goff, S. Maron, A. Fargues, A. Garcia, C. Martineau, F. Taulelle, S. Kahlal, T. Gacoin, J. Boilot, S. Perruchas, *J. Am. Chem. Soc.* 2014, **136**, 11311–11320; (e) W. R. Browne, B. L. Feringa, *Nat. Nanotechnol.* 2006, **1**, 25–35; (f) H. Jintoku, M. Yamaguchi, M. Takafuji, H. Ihara, *Adv. Funct. Mater.* 2014, **24**, 4105–4112.
 - (a) A. Z. Ruiz, H. Li, G. Calzaferri, *Angew. Chem., Int. Ed.* 2006, **45**, 5282–5287; (b) S. S. Babu, V. K. Praveen, A. Ajayaghosh, *Chem. Rev.*, 2014, **114**, 1973–2129; (c) J. Ye, C. Zhang, C. L. Zou, Y. Yan, J. Gu, Y. S. Zhao, J. Yao, *Adv. Mater.* 2014, **26**, 620–624; (d) M. Matsui, M. Fukushima, Y. Kubota, K. Funabiki, M. Shiro, *Tetrahedron*, 2012, **68**, 1931–1935; (e) D. Li, H. Zhang, Y. Wang, *Chem. Soc. Rev.* 2013, **42**, 8416–8433.
 - (a) Y. Che, D. E. Gross, H. Huang, D. Yang, X. Yang, E. Discekici, Z. Xue, H. Zhao, J. S. Moore, L. Zang, *J. Am. Chem. Soc.* 2012, **134**, 4978–4982; (b) M. E. Germain, M. J. Knapp, *J. Am. Chem. Soc.* 2008, **130**, 5422–5423; (c) K. K. Kartha, S. S. Babu, S. Srinivasan, A. Ajayaghosh, *J. Am. Chem. Soc.* 2012, **134**, 4834–4841; (d) B. Xu, X. Wu, H. Li, H. Tong, L. Wang, *Macromolecules* 2011, **44**, pp 5089–5092; (e) Y. Wang, Y. Ni, *Anal. Chem.* 2014, **86**, 7463–7470; (f) H. Luo, S. Chen, Z. Liu, C. Zhang, Z. Cai, X. Chen, G. Zhang, Y. Zhao, S. Decurtins, S. Liu, D. Zhang, *Adv. Funct. Mater.* 2014, **24**, 4250–4258.
 - (a) P. Xue, Q. Xu, P. Gong, C. Qian, A. Ren, Y. Zhang, R. Lu, *Chem. Commun.* 2013, **49**, 5838–5840; (b) Y. Che, L. Zang, *Chem. Commun.*, 2009, 5106–5108; (c) B. Jiang, D. Guo, Y. Liu, *J. Org. Chem.*, 2010, **75**, 7258–7264 (d) B. Jiang, D. Guo, Y. Liu, *J. Org. Chem.* 2011, **76**, 6101–6107 (e) H. Peng, L. Ding, T. Liu, X. Chen, L. Li, S. Yin, Y. Fang, *Chem.–Asian J.* 2012, **7**, 1576–1582; (f) X. Liu, X. Zhang, R. Lu, P. Xue, D. Xu, H. Zhou, *J. Mater. Chem.*, 2011, **21**, 8756–8765; (g) X. Zhang, X. Liu, R. Lu, H. Zhang, P. Gong, *J. Mater. Chem.* 2012, **22**, 1167–1172; (h) L. Shi, Y. Fu, C. He, D. Zhu, Y. Gao, Y. Wang, Q. He, H. Cao, J. Cheng, *Chem. Commun.* 2014, **50**, 872–874; (i) Y. Fu, Q. He, D. Zhu, Y. Wang, Y. Gao, H. Cao, J. Cheng, *Chem. Commun.* 2013, **49**, 11266–11268.
 - (a) P. Xue, R. Lu, P. Zhang, J. Jia, Q. Xu, T. Zhang, M. Takafuji, H. Ihara, *Langmuir* 2013, **29**, 417–425; (b) Y. Li, K. Liu, J. Liu, J. Peng, X. Feng, Y. Fang, *Langmuir* 2006, **22**, 7016–7020; (c) F. Robert-Peillard, E. Palacio-Barco, B. Coulomb, J. L. Boudenne, *Talanta* 2012, **88**, 230–236;
 - (a) Y. Cao, L. Ding, W. Hu, L. Wang, Y. Fang, *Appl. Surf. Sci.* 2013, **273**, 542–548; (b) W. Wang, X. Wang, Q. Yang, X. Fei, M. Sun, Y. Song, *Chem. Commun.* 2013, **49**, 4833–4835 (c) W. Wang, Y. Li,

- M. Sun, C. Zhou, Y. Zhang, Y. Li, Q. Yang, *Chem. Commun.* 2012, **48**, 6040-6042; (d) P. Li, C. Ji, H. Ma, M. Zhang, Y. Cheng, *Chem. -Eur. J.* 2014, **20**, 5741-5745.
7. (a) Y. Tian, B. R. Shumway, D. R. Meldrum, *Chem. Mater.* 2010, **22**, 2069-2078; (b) D. O. Mártire, W. Massad, H. Montejano, M. C. Gonzalez, P. Caregnato, L. S. Villata, N. A. García, *Chem. Pap.* 2014, **68**, 1137-1140; (c) C. S. Smith, K. R. Mann, *J. Am. Chem. Soc.* 2012, **134**, 8786-8789; (d) C. A. Kelly, C. Toncelli, J. P. Kerry, D. B. Papkovsky, *J. Mater. Chem. C* 2014, **2**, 2169-2174; (e) X. Wanga, O. S. Wolfbeis, *Chem. Soc. Rev.* 2014, **43**, 3666-3761.
8. Y. Salinas, R. Martínez-Máñez, M. D. Marcos, F. Sancenón, A. M. Costero, M. Parraad, S. Gil, *Chem. Soc. Rev.* 2012, **41**, 1261-1296.
9. (a) H. Y. Zhang, Z. L. Zhang, K. Q. Ye, J. Y. Zhang, Y. Wang, *Adv. Mater.* 2006, **18**, 2369-2372; (b) Y. Dong, B. Xu, J. Zhang, X. Tan, L. Wang, J. Chen, H. Lv, S. Wen, B. Li, L. Ye, B. Zou, W. Tian, *Angew. Chem., Int. Ed.* 2012, **51**, 10782-10785.
10. (a) Z. Chi, X. Zhang, B. Xu, X. Zhou, C. Ma, Y. Zhang, S. Liu, J. Xu, *Chem. Soc. Rev.*, 2012, **41**, 3878-3896; (b) X. Zhang, Z. Chi, Y. Zhang, S. Liu, J. Xu, *J. Mater. Chem. C* 2013, **1**, 3376-3390; (c) A. Pucci, G. Ruggeri, *J. Mater. Chem.* 2011, **21**, 8282-8291; (d) M. M. Caruso, D. A. Davis, Q. Shen, S. A. Odom, N. R. Sottos, S. R. White, J. S. Moore, *Chem. Rev.* 2009, **109**, 5755-5798; (e) K. Ariga, T. Mori, J. P. Hill, *Adv. Mater.* 2012, **24**, 158-176; (f) F. Ciardelli, G. Ruggeri, A. Pucci, *Chem. Soc. Rev.*, 2013, **42**, 857-870.
11. (a) Q. Qi, J. Zhang, B. Xu, B. Li, S. X. Zhang, W. Tian, *J. Phys. Chem. C*, 2013, **117**, 24997-25003; (b) T. Han, Y. Zhang, X. Feng, Z. Lin, B. Tong, J. Shi, J. Zhi, Y. Dong, *Chem. Commun.*, 2013, **49**, 7049-7051; (c) X. Zhang, Z. Chi, B. Xu, B. Chen, X. Zhou, Y. Zhang, S. Liu, J. Xu, *J. Mater. Chem.*, 2012, **22**, 18505; (d) C. Li, X. Luo, W. Zhao, C. Li, Z. Liu, Z. Bo, Y. Dong, Y. Dong, B. Z. Tang, *New J. Chem.* 2013, **37**, 1696-1699; (e) X. Luo, W. Zhao, J. Shi, C. Li, Z. Liu, Z. Bo, Y. Q. Dong, B. Z. Tang, *J. Phys. Chem. C* 2012, **116**, 21967-21972; (f) X. Luo, J. Li, C. Li, L. Heng, Y. Q. Dong, Z. Liu, Z. Bo, B. Z. Tang, *Adv. Mater.*, 2011, **23**, 3261-3265; (g) X. Zhang, Z. Chi, H. Li, B. Xu, X. Li, W. Zhou, S. Liu, Y. Zhang, J. Xu, *Chem. - Asian J.* 2011, **6**, 1470-1478; (h) R. H. Pawle, T. E. Haas, P. Müller, S. W. Thomas III, *Chem. Sci.*, 2014, DOI: 10.1039/C4SC01466A; (i) R. Li, S. Xiao, Y. Li, Q. Lin, R. Zhang, J. Zhao, C. Yang, K. Zou, D. Liam, T. Yi, *Chem. Sci.*, 2014, DOI: 10.1039/C4SC01243G.
12. P. Xue, B. Yao, J. Sun, Z. Zhang, R. Lu, *Chem. Commun.* 2014, **50**, 10284-10286.
13. P. Xue, B. Yao, J. Sun, Z. Zhang, K. Li, B. Liu, R. Lu, *Dyes Pigments* 2015, **112**, 255-261.
14. (a) Z. Song, Y. Hong, R. T. K. Kwok, J. W. Y. La, B. Liu, B. Z. Tang, *J. Mater. Chem. B* 2014, **2**, 1717-1723; (b) J. Huang, R. Tang, T. Zhang, Q. Li, G. Yu, S. Xie, Y. Liu, S. Ye, J. Qin, Z. Li, *Chem. Eur. J.* 2014, **20**, 5317-5326; (c) Y. Liao, K. Li, M. Wu, T. Wu, X. Yu, *Org. Biomol. Chem.* 2014, **12**, 3004-3008.
15. (a) P. Xue, P. Chen, J. Jia, Q. Xu, J. Sun, B. Yao, Z. Zhang, R. Lu, *Chem. Commun.* 2014, **50**, 2569-2571; (b) A. Mishra, S. Chatterjee, G. Krishnamoorthy, *J. Photochem. Photobiol. A Chem.* 2013, **260**, 50-58; (c) Fayed, T. A. *J. Photochem. Photobiol. A Chem.* 1999, **121**, 17-25.
16. (a) P. Xue, R. Lu, J. Jia, M. Takafuji, H. Ihara, *Chem. Eur. J.* 2012, **18**, 3549-3558; (b) C. F. G. C. Geraldes, A. D. Sherry, M. P. M. Marques, M. C. Alpoim, S. Cortes, *J. Chem. Soc., Perkin Trans.* 1991, **2**, 137-146; (c) K. Wang, S. Huang, Y. Zhang, S. Zhao, H. Zhang and Y. Wang, *Chem. Sci.*, 2013, **4**, 3288-3293; (d) D. Liu, Z. Zhang, H. Zhang and Y. Wang, *Chem. Commun.*, 2013, **49**, 10001-10003.
17. (a) F. Würthner, T. E. Kaiser, C. R. Saha-Möller, *Angew. Chem., Int. Ed.* 2011, **50**, 3376-3410; (b) H. Jintoku, M. Yamaguchi, M. Takafuji, H. Ihara, *Adv. Funct. Mater.* 2014, **24**, 4105-4112; (c) H. Jintoku, H. Ihara, *Chem. Commun.* 2012, **48**, 1144-1146.
18. (a) R. Hu, J. W. Y. Lam, H. Deng, Z. Song, C. Zheng, B. Z. Tang, *J. Mater. Chem. C* 2014, **2**, 6326-6332; (b) P. Xue, R. Lu, G. Chen, Y. Zhang, H. Nomoto, M. Takafuji, H. Ihara, *Chem. Eur. J.* 2007, **13**, 8231 - 8239; (c) R. Hu, N. L. C. Leung, B. Z. Tang, *Chem. Soc. Rev.*, 2014, **43**, 4494-4562.
19. (a) S. Yoon, S. Varghese, S. K. Park, R. Wannemacher, J. Gierschner, S. Y. Park, *Adv. Opt. Mater.* 2013, **1**, 232-237 (b) J. Gierschner, S. Y. Park, *J. Mater. Chem. C* 2013, **1**, 5818-5832.
20. (a) C. Ma, B. Xu, G. Xie, J. He, X. Zhou, B. Peng, L. Jiang, B. Xu, W. Tian, Z. Chi, S. Liu, Y. Zhang, J. Xu, *Chem. Commun.* 2014, **50**, 7374-7377; (b) J. Zhang, J. Chen, B. Xu, L. Wang, S. Ma, Y. Dong, B. Li, L. Ye, W. Tian, *Chem. Commun.* 2013, **49**, 3878-3880.
21. (a) C. Wang, S. Chen, K. Wang, S. Zhao, J. Zhang, Y. Wang, *J. Phys. Chem. C* 2012, **116**, 17796-17806; (b) G. Zhang, J. Lu, M. Sabat, C. L. Fraser, *J. Am. Chem. Soc.* 2010, **132**, 2160-2162; (c) K. Nagura, S. Saito, H. Yusa, H. Yamawaki, H. Fujihisa, H. Sato, Y. Shimoikeda, S. Yamaguchi, *J. Am. Chem. Soc.* 2013, **135**, 10322-10325; (d) A. E. Metz, E. E. Podlesny, P. J. Carroll, A. N. Klinghoffer, M. C. Kozlowski, *J. Am. Chem. Soc.* 2014, **136**, 10601-10604; (e) W. Ni, Y. Qiu, M. Li, J. Zheng, R. W. Sun, S. Zhan, S. W. Ng, D. Li, *J. Am. Chem. Soc.* 2014, **136**, 9532-9535; (f) Y. Gong, Y. Zhang, W. Z. Yuan, J. Z. Sun, Y. Zhang, *J. Phys. Chem. C* 2014, **118**, 10998-11005; (g) M. Yuan, D. Wang, P. Xue, W. Wang, J. Wang, Q. Tu, Z. Liu, Y. Liu, Y. Zhang, J. Wang, *Chem. Mater.* 2014, **26**, 2467-2477; (h) M. Krikorian, S. Liu, T. M. Swager, *J. Am. Chem. Soc.* 2014, **136**, 2952-2955.
22. (a) Z. Ma, M. Teng, Z. Wang, S. Yang, X. Jia, *Angew. Chem. Int. Ed.* 2013, **52**, 12268 -12272; (b) P. Xue, B. Yao, J. Sun, Q. Xu, P. Chen, Z. Zhang, R. Lu, *J. Mater. Chem. C* 2014, **2**, 3942-3950; (c) Y. Sagara, T. Mutai, I. Yoshikawa, Araki, K. *J. Am. Chem. Soc.* 2007, **129**, 1520-1521.
23. N. Mizoshita, T. Tani, S. Inagaki, *Adv. Mater.* 2012, **24**, 3350-3355.
24. X. Luo, J. Li, C. Li, L. Heng, Y. Q. Dong, Z. Liu, Z. Bo, B. Z. Tang, *Adv. Mater.* 2011, **23**, 3261-3265.
25. (a) G. Zhang, H. Wang, M. P. Aldred, T. Chen, Z. Chen, X. Meng, M. Zhu, *Chem. Mater.* 2014, **26**, 4433-4446; (b) Y. Zhang, T. Han, S. Gu, T. Zhou, C. Zhao, Y. Guo, X. Feng, B. Tong, J. Bing, J. Shi, J. Zhi, Y. Dong, *Chem. Eur. J.* 2014, **20**, 8856-8861.